ELECTRON BEAM CHARGING AND ARC DISCHARGING OF SPACECRAFT INSULATING MATERIALS

Final Report
Period: 1 Oct. 1979 to 30 Sept. 1980
NASA Grant NSG-7647
Submitted to NASA Lewis Research Center
21000 Brookpark Road, Cleveland, Ohio

October 1980

K.G. Balmain
Department of Electrical Engineering
University of Toronto
Toronto, Canada M5S 1A4

Funding agencies:
U.S. Air Force Weapons Laboratory
U.S. National Aeronautics and Space Administration

ELECTRON BEAM CHARGING AND ARC DISCHARGING OF SPACECRAFT INSULATING MATERIALS

Final Report
Period: 1 Oct. 1979 to 30 Sept. 1980
NASA Grant NSG-7647
Submitted to NASA Lewis Research Center
21000 Brookpark Road, Cleveland, Ohio

October 1980

K.G. Balmain
Department of Electrical Engineering
University of Toronto
Toronto, Canada M5S 1A4

Funding agencies:
U.S. Air Force Weapons Laboratory
U.S. National Aeronautics and Space Administration

ABSTRACT

This final report deals with the properties of the arc discharges which are caused by the laboratory exposure of dielectric materials to electron beams, the intent being to simulate conditions on synchronous-orbit spacecraft. Extensive experimental studies are reported for planar dielectrics (Teflon, Kapton,Mylar) on the subjects of incident-flux scaling of discharge properties and the effects of high-energy broad-spectrum electron irradiation from a radioisotope source. In addition a preliminary evaluation is made of the discharge susceptibility of fiber-optic waveguides.

ACKNOWLEDGMENT

Numerous suggestions from W.G. Kuller were very helpful in both experiment planning and interpretation.

PERSONNEL

K.G. Balmain, Professor and Principal Investigator

W. Hirt, Research Engineer

G.R. Dubois, Engineering Technologist

P.C. Kremer, Engineering Technologist

R.D. Reeves, Graduate Student

PUBLICATION OF NASA GRANT RESEARCH RESULTS

1. K.G. Balmain and W. Hirt, "Dielectric Surface Discharges: Dependence on Incident Electron Flux"; presented at the IEEE Conference on Nuclear and Space Radiation Effects, Cornell University, July 1980, and accepted for publication in the IEEE Transactions on Nuclear Science, Vol. NS-27, No. 6, December 1980.

2. K.G. Balmain and W. Hirt, "Dielectric Surface Discharges: Effects of Combined Low-Energy and High-Energy Incident Electrons"; accepted for presentation at the Spacecraft Charging Technology Conference III, Colorado Springs, November 1980, and scheduled to appear in the Proceedings of that conference.

OTHER RELEVANT PUBLICATIONS DURING 1979-1980

1. K.G. Balmain and G.R. Dubois, "Surface Discharges on Teflon, Mylar and Kapton", IEEE Trans. Nucl. Sci., Vol. NS-26, No. 6, Dec. 1979, pp. 5146-5151.

2. K.G. Balmain, "Surface Discharge Arc Propagation and Damage on Spacecraft Dielectrics", Proceedings of the ESA Symposium on Spacecraft Materials, ESA Publication No. SP-145, December 1979, pp. 209-215.

3. K.G. Balmain, "Surface Discharge Effects", AIAA Progress in Astronautics and Aeronautics, Vol. 71, 1980, pp. 276-298.

TABLE OF CONTENTS

1. SUMMARY OF PROGRESS

The scaling of dielectric surface discharges with incident 20 keV electron flux has been studied using planar specimens of Teflon, Kapton and Mylar. Among these materials, Kapton is the only one exhibiting any scaling with incident flux. The degree of scaling is sufficient to require its being taken into account in any estimate of the charging threat to spacecraft. Nevertheless because the scaling law is now known, accelerated testing at high incident current densities appears to be feasible.

A study has been made of the effect on dielectric surface discharges of adding high energy electrons to a primary 20 keV, 10 nA/cm^2 electron beam, the high-energy broad-spectrum particles coming from the β-decay of Strontium - 90. Kapton exhibits the most surprising effect, which is significantly increased discharge strength, increased waiting time between discharges, and a decreased number of discharges per specimen before discharge cessation. Mylar exhibits similar but less pronounced effects, while Teflon is relatively unaffected. There is evidence that with Kapton and Mylar the high energy electrons act in some way to delay the instant of discharge ignition so that more charge can be accumulated and hence released during discharge.

Three types of commercial fiber-optic waveguide have been studied with respect to surface discharge susceptibility. Discharges were initiated readily only when a metal edge was in contact with the fiber and then only for incident current densities appreciably higher than required for discharges on the planar dielectrics tested. Coupling of light from the discharge into the fiber occurred only for an all-plastic fiber with extremely thin cladding.

2. DIELECTRIC SURFACE DISCHARGES: DEPENDENCE ON INCIDENT ELECTRON FLUX

2.1 Introduction

It has been reported[1] that the properties of Kapton surface discharge arcs are dependent on the incident electron flux, in particular that the released charge can be roughly linearly proportional to the incident electron current density and that the peak discharge current also increases with increasing incident-beam current density. In the same paper it was also noted that a second-surface mirror array and a fiberglass specimen did not exhibit the same behavior. This incident flux dependence is very important in estimating the probable strength of discharges on spacecraft in synchronous orbit. It is also crucial in determining the relevance to spacecraft considerations of laboratory experiments carried out at the relatively high incident electron beam current densities which are useful for accelerated testing[2].

In the flux-dependence experiments referred to above[1], realistic large-area dielectric specimens were used, but the number of values of incident current densities employed was too small to get an accurate measure of the scaling laws which are applicable. Furthermore, existing information does not indicate whether or not other polymers used in space behave in the same way as Kapton. The experiments to be described in this paper were designed to provide the information referred to above, and also to provide additional data on the division of discharge current between the metal substrate and the metal mask used to define the exposed area.

2.2 The Experiment

The experimental arrangement is depicted in Fig. 1. The materials used were Kapton H with a vacuum-deposited aluminum backing, and Mylar and FEP Teflon without metallixation, the three materials having thicknesses of 50 μm, 75 μm and 50 μm respectively. The incident beam energy was fixed at 20 keV and the beam uniformity over the exposed area was better than ±20% as measured by an array of five Faraday cups before and after the experiments; also, continuous monitoring with a single Faraday cup was provided during the experiments. The range of incident current densities used was 0.5 to 100 nA/cm^2. The exposed dielectric area was 11.7 cm^2 as defined by a circular aperture in a 1.6 mm thick aluminum mask, the aperture having a 45° bevelled edge to reduce emitted electron interception. The outer dimensions of the mask and substrate were 8 x 9 cm, making the exposed dielectric area appreciably smaller than the exposed mask area, in contrast to previous experiments[1] involving a very narrow edge clamp (equivalent to the mask). The measurement system employed a two-channel 400 MHz bandwidth oscilloscope connected through appropriate attenuators to the specimen substrate and mask, each shunted to ground with a 2.5 ohm load resistor made up of 8 low-inductance 20 ohm half-watt resistors in parallel.

2.3 Results for Kapton H

The substrate discharge current pulse is characterized by its peak

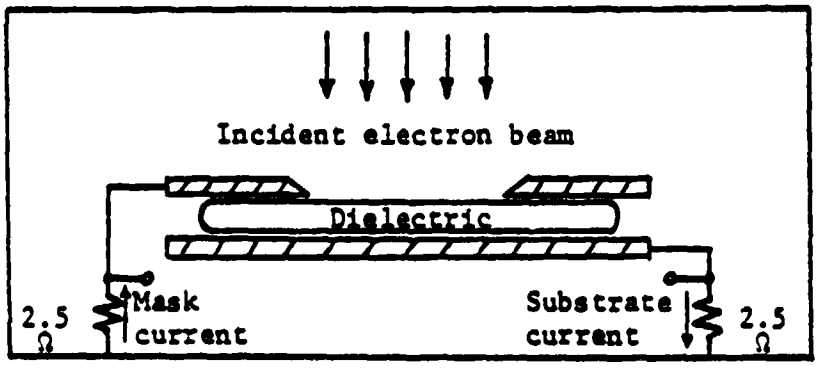

Fig. 1

Experimental arrangement in vacuum chamber

current, released charge and duration, the latter two defined as

$$Q_s = \int I_s(t)\, dt \tag{1}$$

$$T_s = \frac{1}{I_s} \int I_s(t)\, dt = \frac{Q_s}{I_s} \tag{2}$$

in which I_s is the peak current. The energy disipated in the substrate load resistor R is

$$E_s = R \int I_s^2(t)\, dt \tag{3}$$

Exactly the same formulas are used to characterize the mask current pulse, namely I_m, Q_m, T_m and E_m .

Figure 2 shows that I_s and Q_s exhibit a definite tendency to decrease with decreasing incident current density. This tendency is appreciably more graduai than one might expect from the previous results[1]. Furthermore, if one were to select only the strongest pulses observed in the range 1-10 nA/cm^2 (the tops of the vertical bars indicating measurement ranges), one would conclude that there is no significant incident-flux dependence at all. However the points representing average values and the best-fit straight line probably provide better guidance for estimating overall trends.

Also shown in Fig. 2 is the pulse duration T_s which is very nearly constant, the indicated slope being small in relation to the indicated measurement ranges. This result is consistent with the notion that the

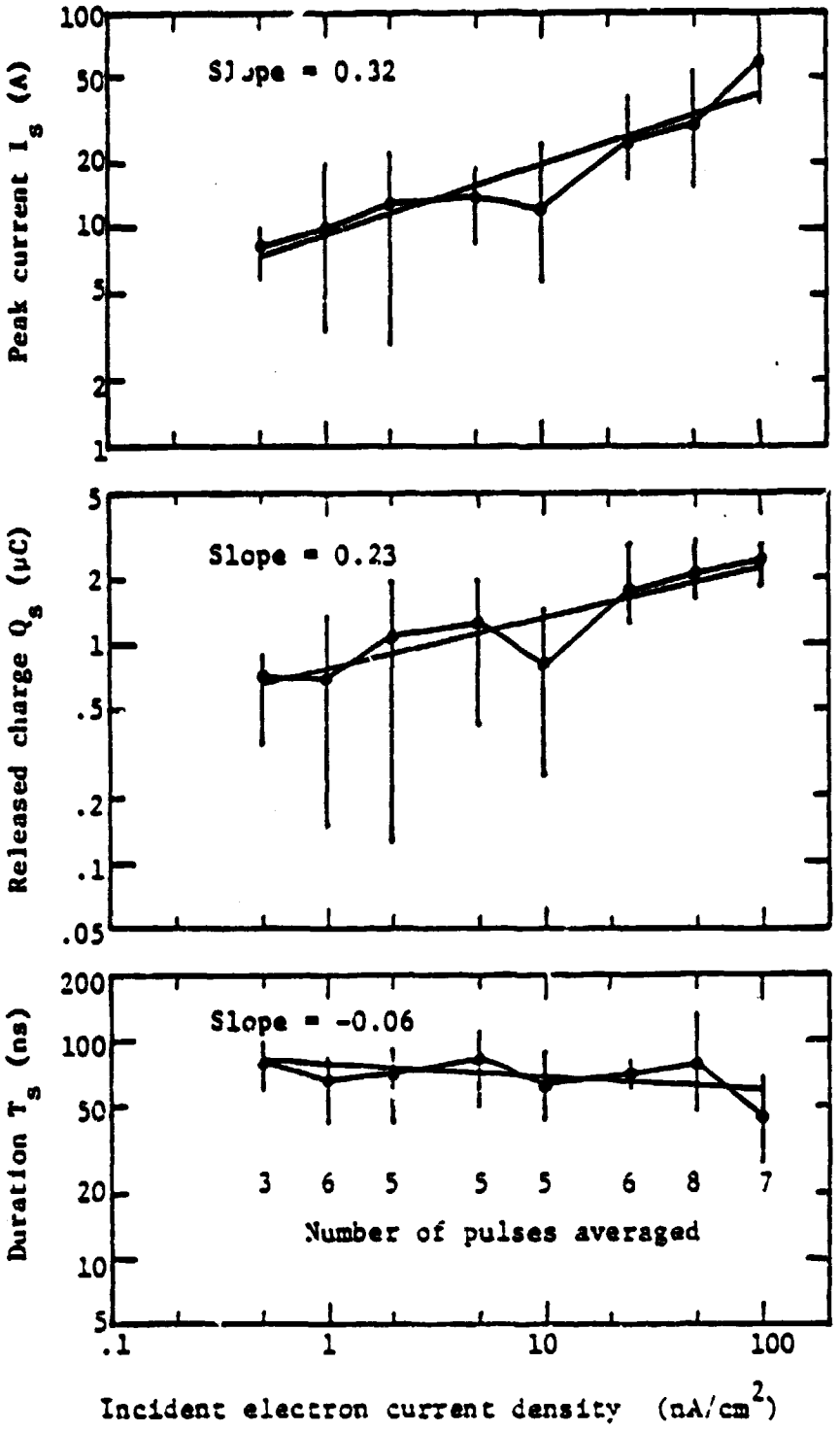

Fig. 2 Substrate discharge current pulse properties for Kapton H. Beam energy = 20 keV, specimen area = 11.7 cm^2, specimen thickness = 50 μm.

pulse duration is determined by the specimen dimensions, because the discharge propagates at a well-defined velocity. This velocity can be estimated by dividing the aperture radius by the pulse duration, which gives 2.6×10^5 m/s.

Similar results for the mask current pulse are given in Fig. 3. The mask current pulse duration gives a discharge propagation velocity of 3.2×10^5 m/s. The energy dissipated in the load resistors attached to both substrate and mask are shown in Fig. 4 which indicates a very significant variation over the range of incident current densities.

As a check, these results for Kapton can be compared with previous results[2] for which the mask was connected directly to the substrate, causing the mask current to bypass the substrate load resistor. In the previous measurements at 80 nA/cm^2 and 11.7 cm^2, the straight-line-interpolated peak current was 20A. In the present measurements, the corresponding current would be the substrate current of 40A minus the mask current of 23A giving 17A, so the comparison in this case is very close.

2.4 Results for Mylar and FEP Teflon

Figures 5 and 6 display the substrate and mask pulse characteristics I, Q, T and E for both Mylar and Teflon. Not one of these characteristics displays any significant variation with incident-beam current density. In the four graphs presented, only the peak current graphs have straight-line approximations all with slope of the same sign (positive in this case).

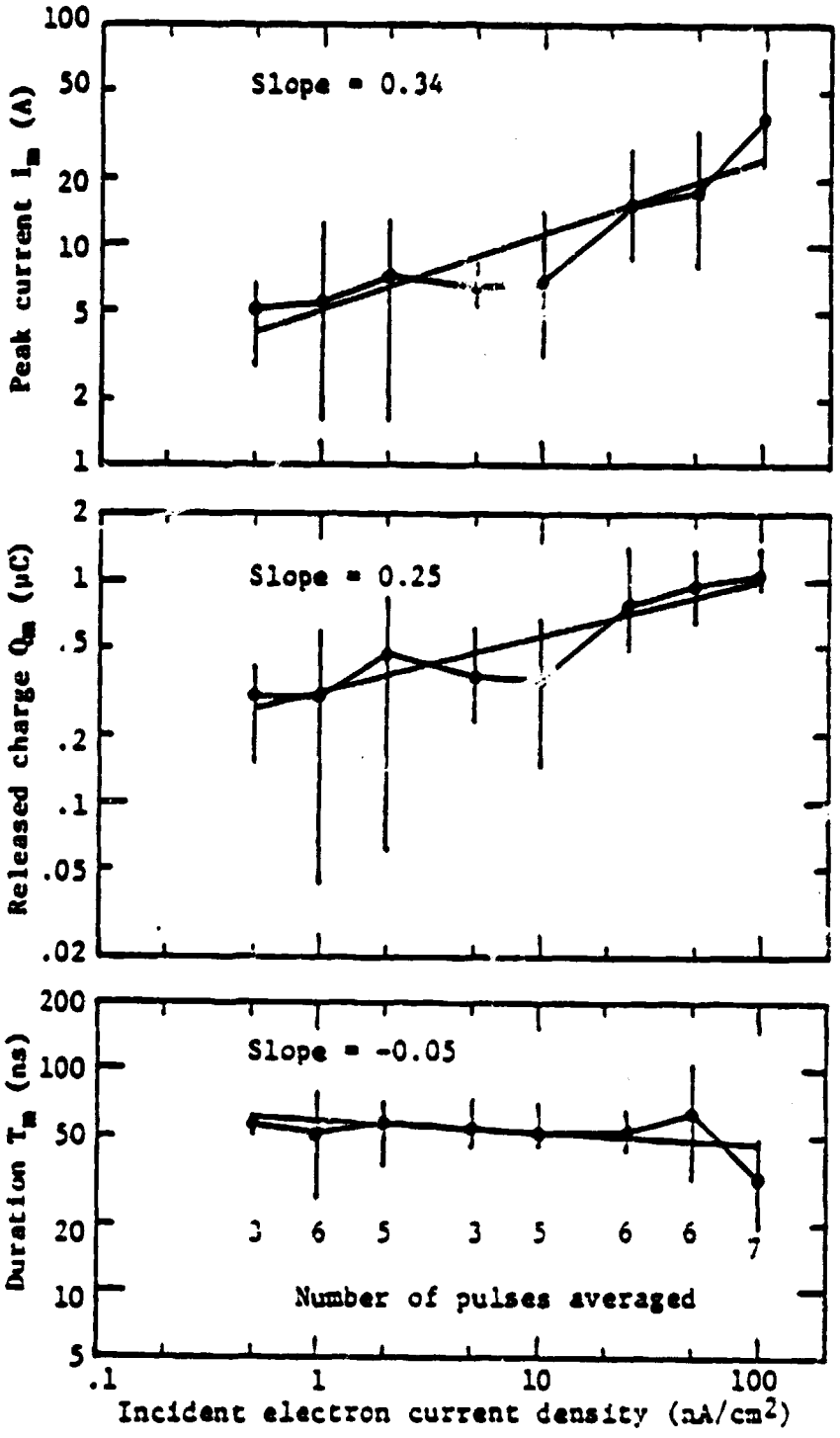

Fig. 3 Mask discharge current pulse properties for Kapton H. Beam energy = 20 keV, specimen area = 11.7 cm^2, specimen thickness = 50 μm.

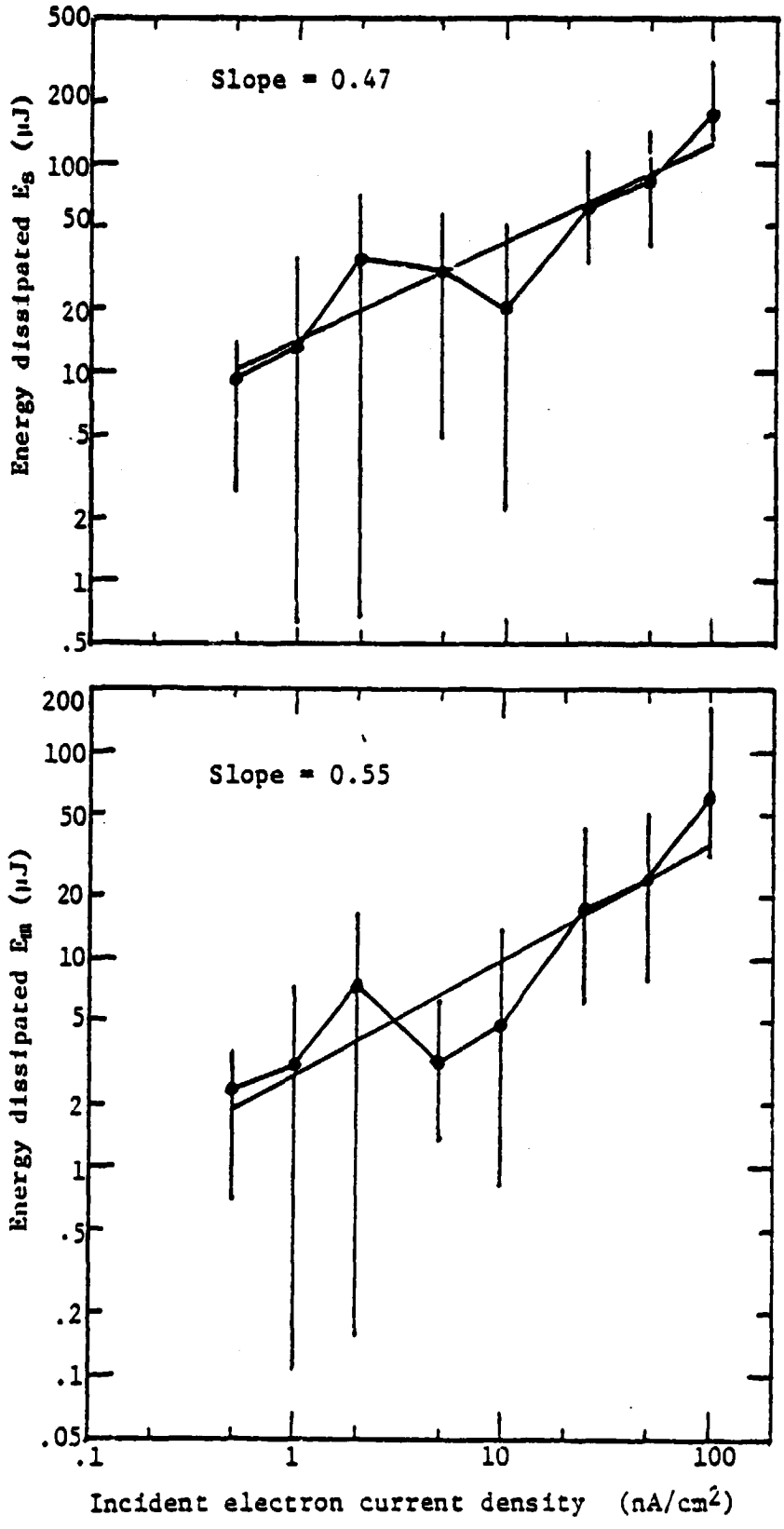

Fig. 4 Substrate (top) and mask (bottom) discharge energy dissipated in a 2.5 ohm resistor for Kapton H. Beam energy = 20 keV, specimen area = 11.7 cm^2, specimen thickness = 50 μm.

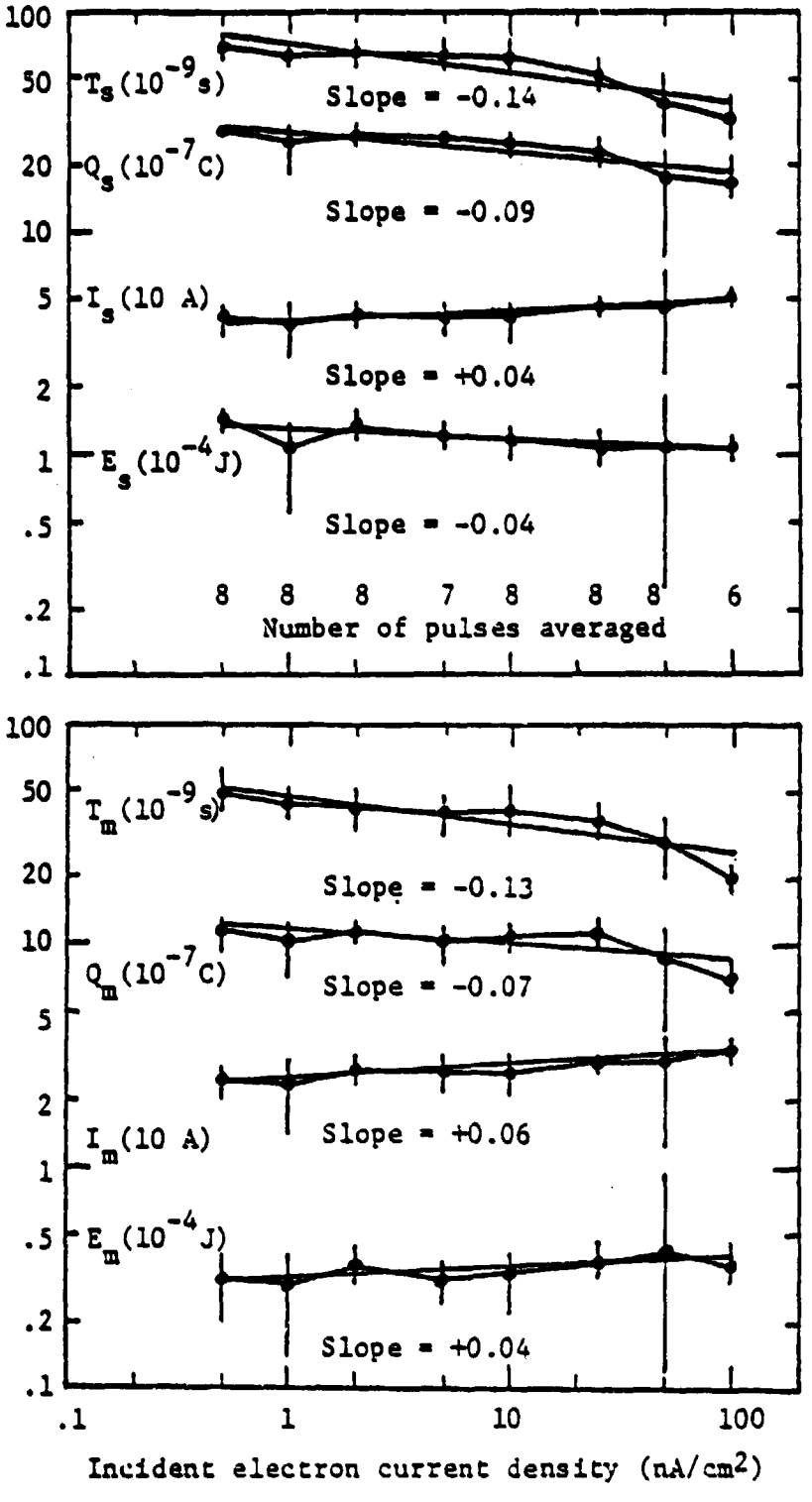

Fig. 5 Substrate (top) and mask (bottom) discharge pulse properties for Mylar. Beam energy = 20 keV, specimen area = 11.7 cm^2, specimen thickness = 75 μm.

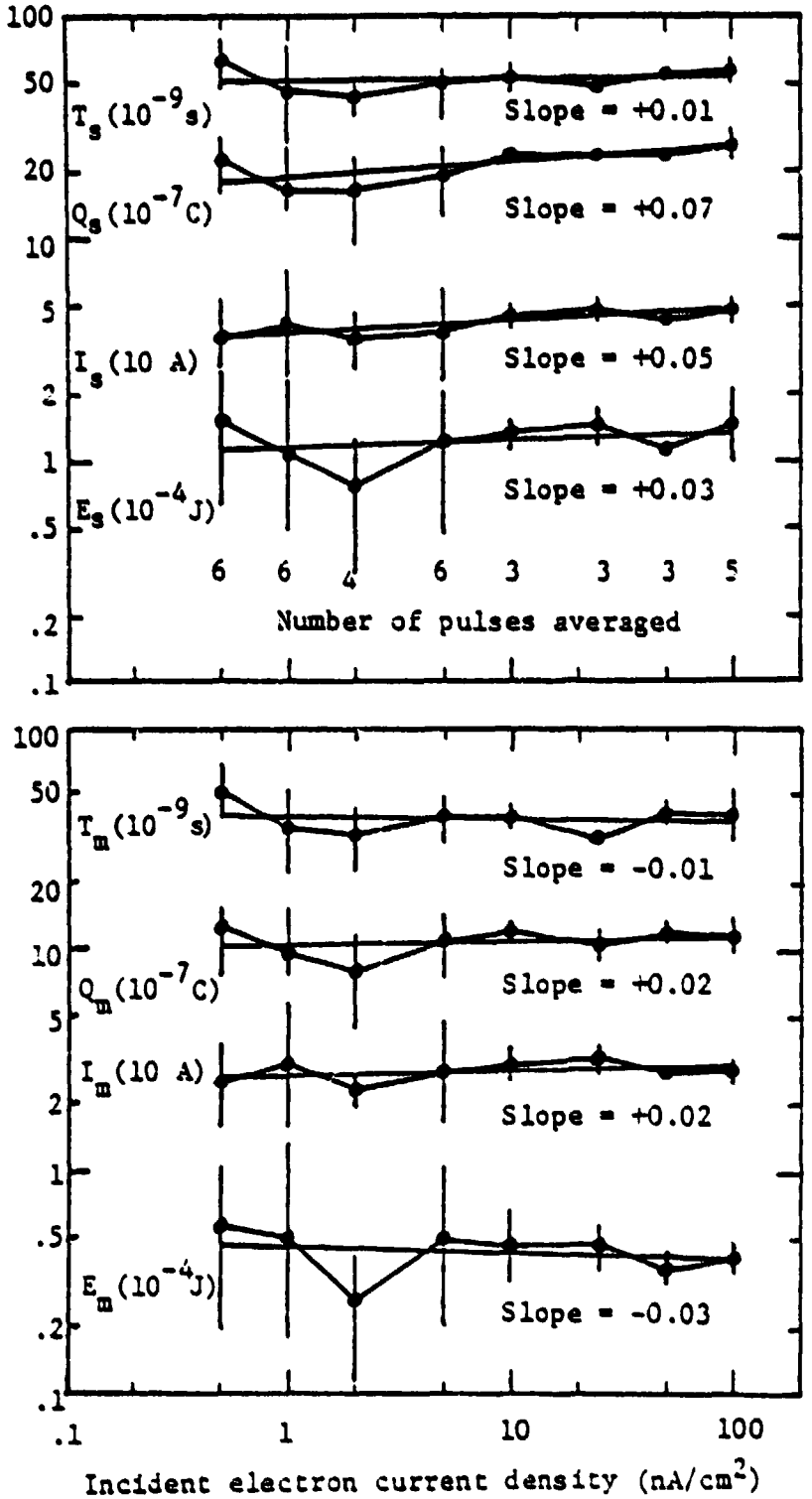

Fig. 6 Substrate (top) and mask (bottom) discharge pulse properties for FEP Teflon. Beam energy = 20 keV, specimen area = 11.7 cm^2, specimen thickness = 50 μm.

2.5 Mask-to-Substrate Ratios

Figures 7, 8 and 9 provide details of the mask-to-substrate ratios for the four averaged pulse characteristics and the three materials. There appears to be no significant flux scaling, although it is interesting to note that all the straight-line approximations for Teflon have negative slopes, while all those for Mylar and Kapton have positive slopes.

To interpret the mask-to-substrate ratios, let us postulate that the discharges are initiated very close to the mask edge where charge concentrations and fields are highest. The surface arcs then propagate inward and die out in the central region of the specimen, a further postulate which is consistent with the appearance of the arcs although their evolution in time has not been measured. As the arc propagates inward, it is reasonable to expect that more of its ejected electrons go to the chamber wall and fewer to the mask. Therefore the mask current pulse should decay more rapidly than the substrate current pulse. In effect this would shorten the mask pulse, as observed.

It is noted that the mask-to-substrate ratios are ordered $I_m/I_s > Q_m/Q_s > E_m/E_s$. To interpret this ordering, suppose that a current pulse consists of an instantaneous rise followed by an exponential decay. That is, take the currents to be zero for $t<0$, and then for $t\geq 0$ take $I_s(t) = e^{-at}$ and $I_m(t) = ke^{-abt}$. The factor k allows for the smaller mask peak current and the factor b allows for the more rapid mask current decay. Equations (1), (2) and (3) then permit derivation of $I_m/I_s = k$, $Q_m/Q_s = k/b$, $E_m/E_s = k^2/b$, and $T_m/T_s = 1/b$. For the given conditions $k<1$ and $b>1$, it is clear that $k>k/b>k^2/b$, or in other words $I_m/I_s > Q_m/Q_s > E_m/E_s$ as observed.

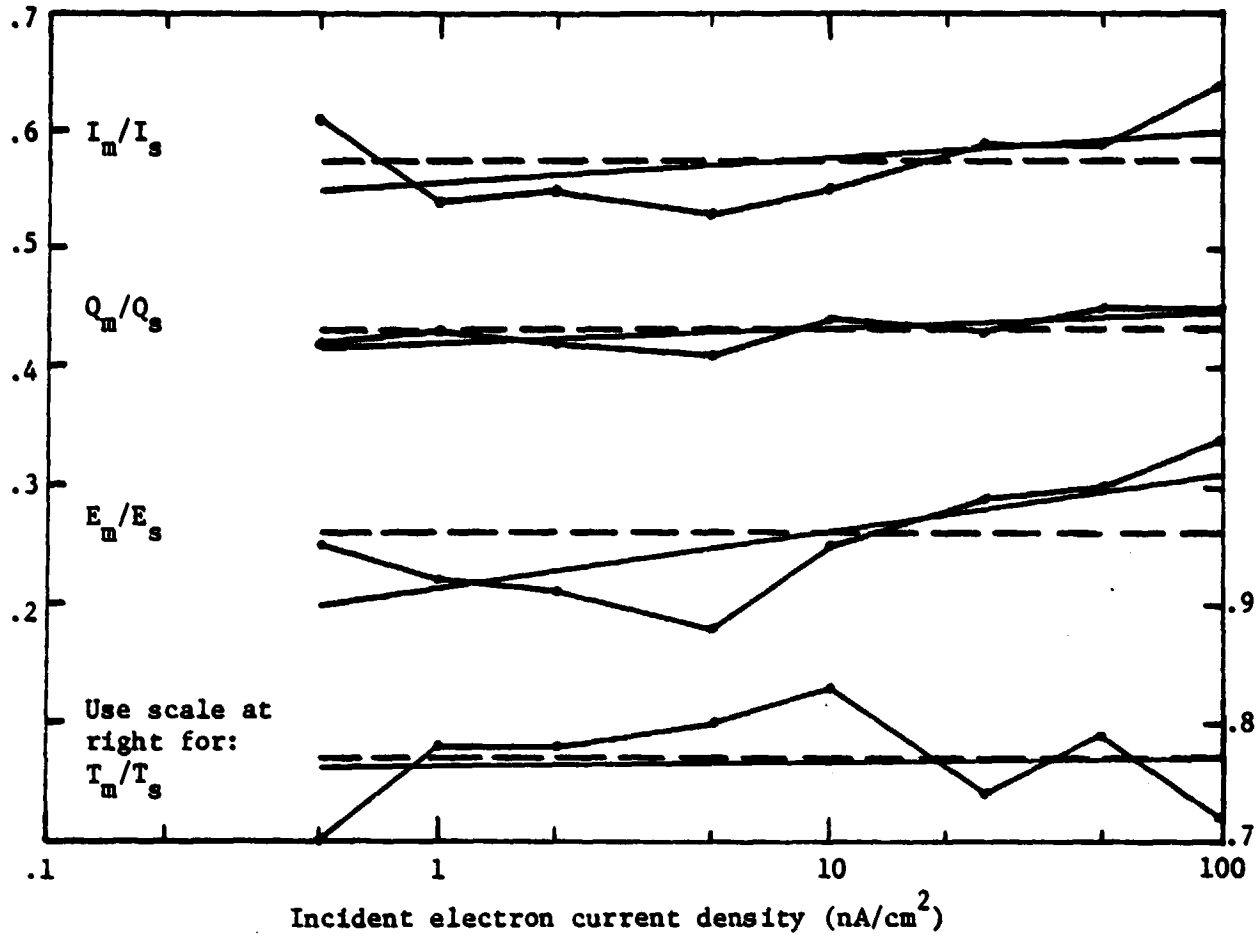

Fig. 7 Mask-to-substrate ratios for Kapton H. Dashed lines are averages and solid lines are best-fit straight lines.

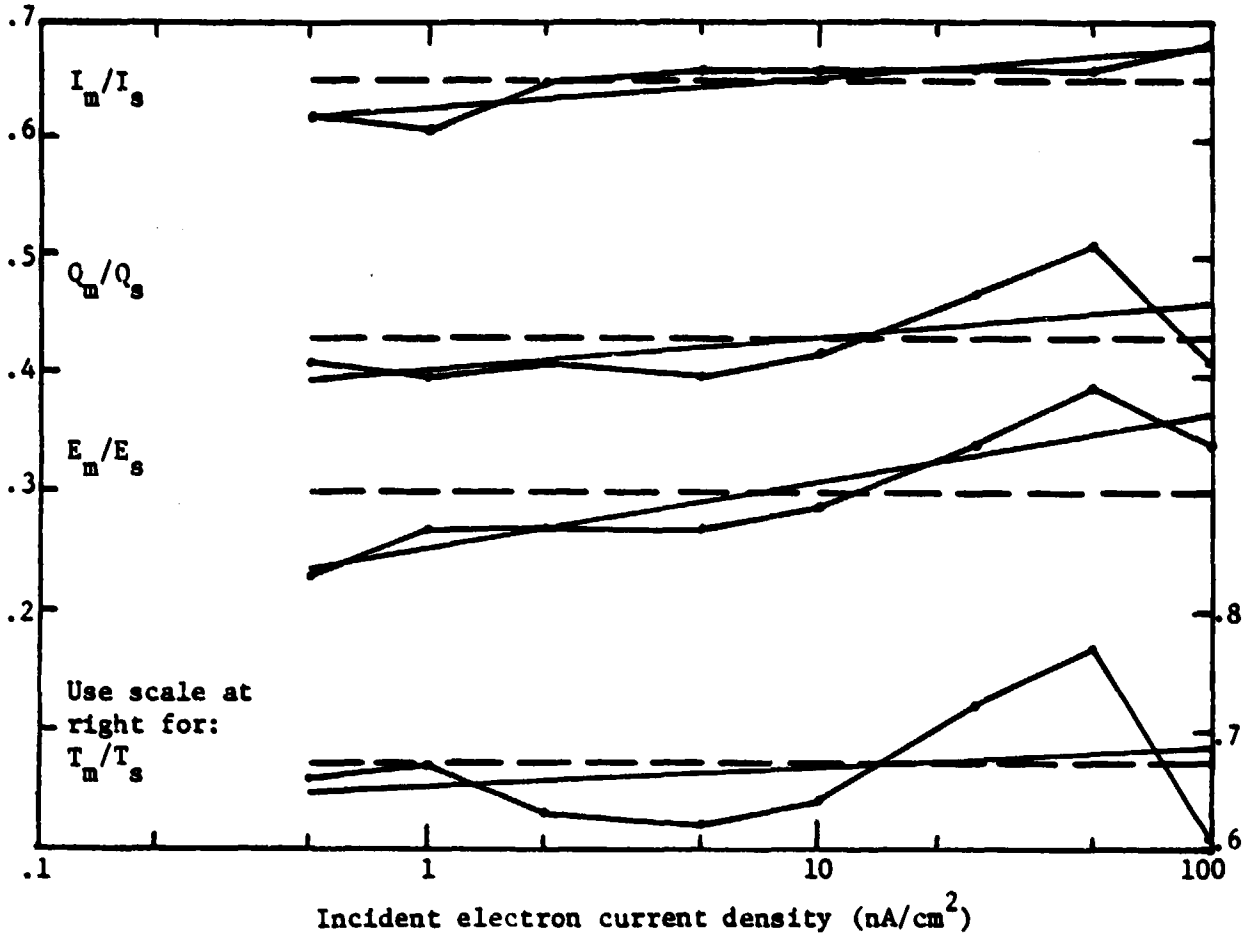

Fig. 8 Mask-to-substrate ratios for Mylar. Dashed lines are averages and solid lines are best-fit straight lines.

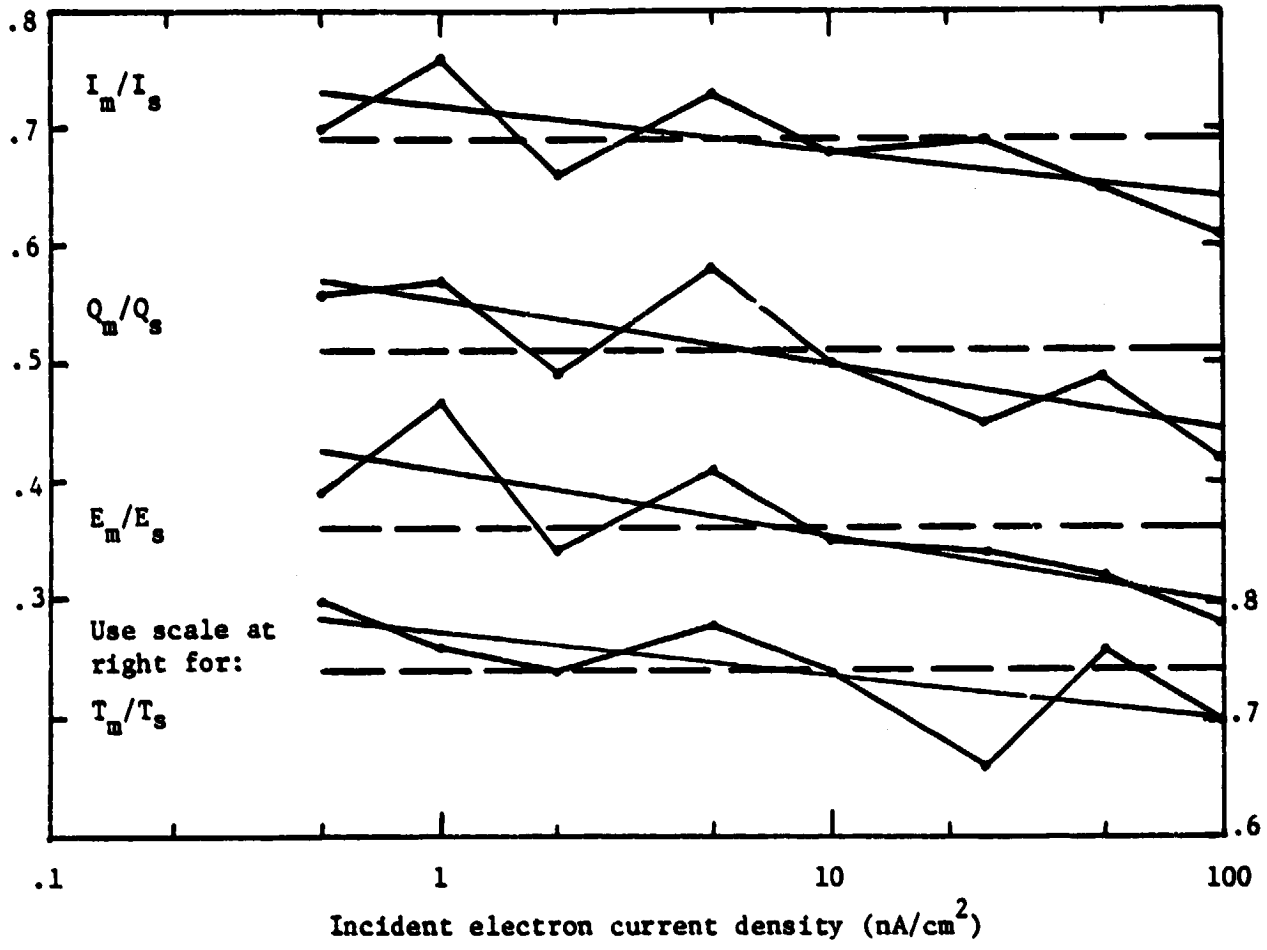

Fig. 9 Mask-to-substrate ratios for FEP Teflon. Dashed lines are averages and solid lines are best-fit straight lines.

The above formulas also suggest that the charge and energy ratios may be deduced from the peak current and duration ratios. This may be tested readily by using the average measured values from Figs. 7, 8 and 9, as indicated in the following table:

Material	I_m/I_s measured	T_m/T_s measured	Q_m/Q_s meas.(calc.)	E_m/E_s meas.(calc.)
Kapton H	.575	.77	.43(.443)	.26(.255)
Mylar	.65	.67	.43(.436)	.30(.283)
FEP Teflon	.69	.74	.51(.511)	.36(.352)

It should also be noted that by definition $T_s = Q_s/I_s$ and $T_m = Q_m/I_m$, so that $Q_m/Q_s = (T_m/T_s)(I_m/I_s)$ which is always less than I_m/I_s as long as $T_m<T_s$, for any pulse model.

In a foregoing paragraph it was postulated that the apparent shortening of the mask pulse might be due to electrons from the central region of the specimen never reaching the mask. The size of this central region can be estimated by starting with the notion that the propagation velocity v_p must be given by $v_p = r_s/T_s = r_m/T_m$ where r_s is the aperture radius and r_m is the arc length over which emitted electrons can reach the mask. This gives $r_m = r_s(T_m/T_s)$. If r_c is the radius of the central region referred to above, then $r_s = r_c + r_m$, from which $r_c/r_s = 1 - (T_m/T_s)$. Data from the above table gives r_c/r_s approximately in the range 1/4 to 1/3. Therefore it would appear that there exists a central region of significant size, from which emitted electrons do not reach the mask.

2.6 Materials Comparison Summary

The pulse characteristics for the three materials tested are summarized

in Fig. 10 with respect to incident flux dependence. Clearly I, Q and E exhibit well-defined scaling with incident flux for Kapton only and not for Mylar or Teflon. For Kapton, a few measurements were carried out at a current density of 200 nA/cm^2, producing still higher values of I, Q and E, and so leaving unsettled the question as to whether or not saturation was being approached. Previous work[2] had been carried out with an incident current density of 80 nA/cm^2, a value which just happens to give Kapton discharge pulse characteristics almost identical to those of Mylar and Teflon.

Figure 11 shows that the mask I, Q and E are significant fractions of the substrate values. Furthermore this figure shows that for Teflon alone, the mask I, Q, E and T all increase with decreasing incident current density, relative to the substrate values. At the lowest incident current density the mask-to-substrate ratio of energy dissipated in the load resistor for Teflon would be approximately twice the value for either Kapton or Mylar, as deduced from the straight-line approximations in Fig. 11.

2.7 Waiting-Time Between Discharges

As the incident current density is decreased, one would expect to wait longer for each discharge to occur, and this is what one finds in the course of performing discharge experiments[3]. For 75 μm thick Mylar, typical waiting-times were 60, 15 and 2.5 minutes for current densities of 0.5, 5 and 50 nA/cm^2. For 50 μm thick Teflon, waiting-times were approximately equal to those for Mylar. For 50 μm thick Kapton, waiting-times varied from 30 to 2.5 minutes for current densities from 0.5 to 50 nA/cm^2.

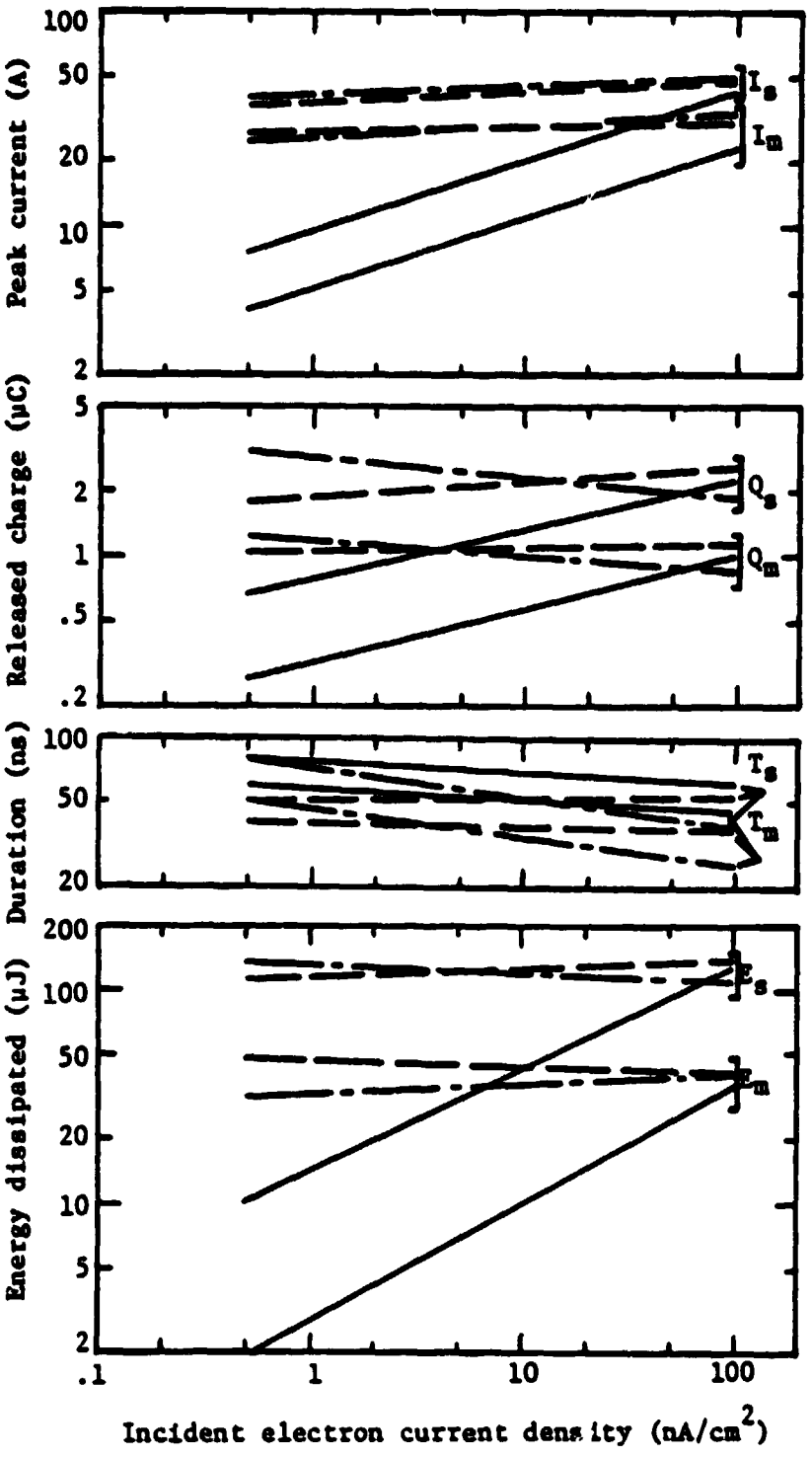

Fig. 10 Comparison of best-fit straight lines for discharge properties of three materials:

Kapton H
Mylar
FEP Teflon

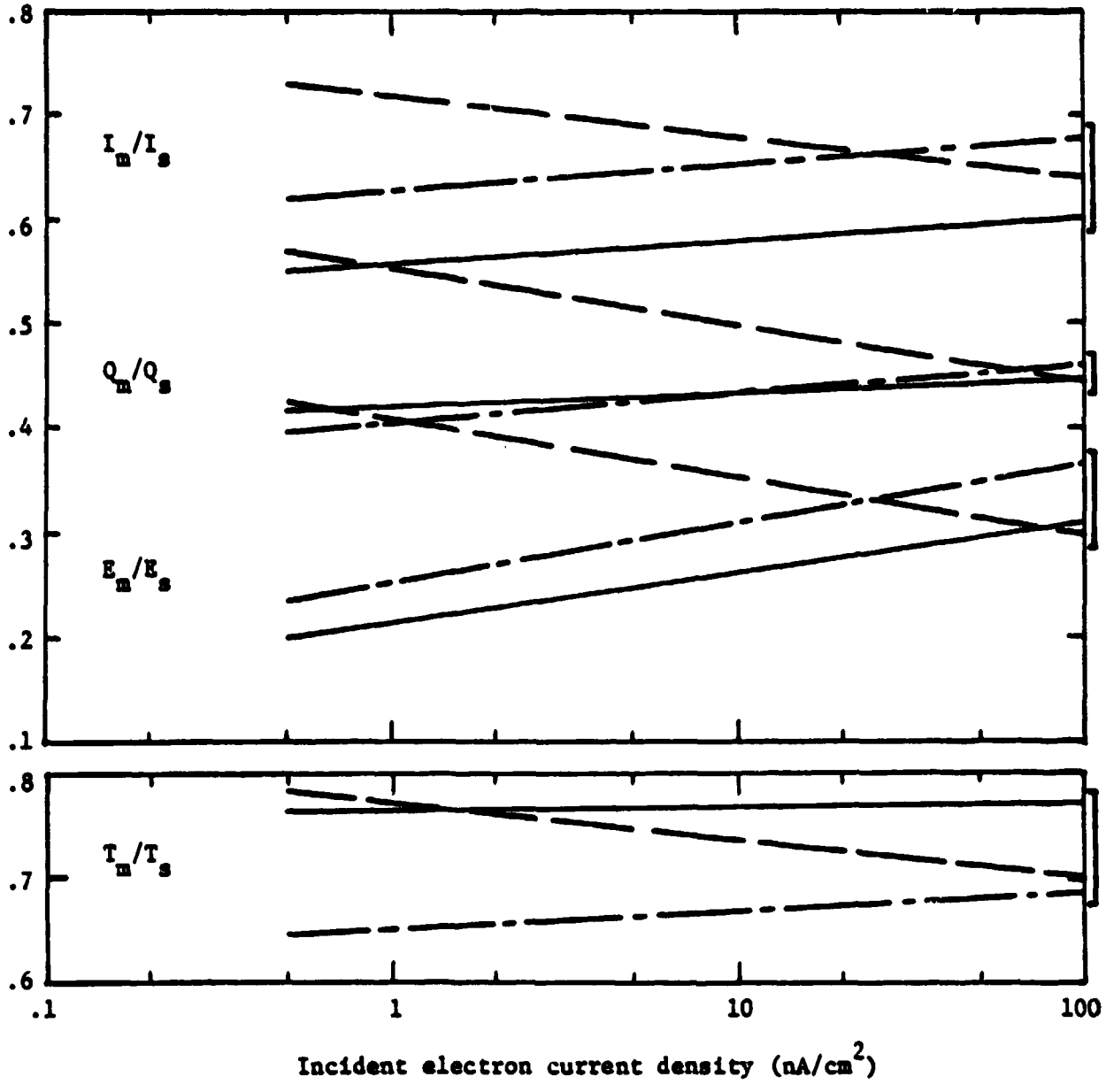

Fig. 11 Comparison of best-fit straight lines for mask-to-substrate ratios of three materials:

Kapton H ——————
Mylar ——·——·——
FEP Teflon — — — —

2.8 Specimen Fatigue

A single 75 μm thick Mylar specimen was used for a total of 66 discharges without showing any signs of fatigue such as changes in discharge strength or waiting-time. The 50 μm thick specimens of Kapton and Teflon exhibited much more erratic behavior, however, with several specimens failing to discharge at all at low current densities. Considering only those specimens which did produce discharges, for Kapton the 49 discharges required 11 specimens and for Teflon the 38 discharges required 10 specimens.

This need for frequent specimen changes came about because of specimen fatigue. On 80% of the Kapton and Teflon specimens this fatigue took the form of a cessation in discharge activity after 4 or 5 discharges. On the remaining 20%, "pinholes" or "punchthroughs" developed in the specimen, followed by very rapid but weak discharges of relatively long duration.

2.9 On an Incident Current Density Threshold for Discharge Occurrence

Consider a uniform charged particle beam of current density J, constant particle density N, particle charge e and velocity v, so that J=Nev, and suppose that this beam actually reaches the specimen after penetrating the potential barrier due to embedded charge. Suppose also that J_o and v_o are the values in the beam at some distance from the specimen, or in other words J_o would be the current density measured by a Faraday cup inserted in place of the specimen. Now if V_b and V_s are the beam accelerating voltage and the specimen surface potential, we

have $eV_b = m v_o^2/2$ and $e(V_b - V_s) = m v^2/2$

Thus $$Ne = \frac{J_o}{v_o} = J_o \sqrt{\frac{m}{2eV_b}}$$

and $$J = Nev = J_o \sqrt{\frac{m}{2eV_b}} \sqrt{\frac{2e(V_b - V_s)}{m}}$$

giving $$J = J_o \sqrt{1 - (V_s/V_b)}$$

Now the internal resistance of a specimen of thickness h, area A and resistivity ρ is $R = \rho h/A$ and the surface potential is

$$V_s = RJA = \rho\, h\, J_o \sqrt{1 - (V_s/V_b)} \qquad (4)$$

Defining V_o to be the voltage drop across the specimen if it passed the total measured current density J_o, we have $V_o = \rho\, h\, J_o$.

Squaring equation (4) gives

$$\left[\frac{V_s}{V_o}\right]^2 + \frac{V_s}{V_b} = 1 \qquad (5)$$

Now consider as an example $V_b = 20$ kV, together with $V_s = 13$ kV and $\rho = 10^{13}\,\Omega$ m, suggested in the literature[1] as being appropriate for 50 μm thick Kapton on the point of punchthrough breakdown. Equation (5) gives $J_o = 4.4$ nA/cm^2 as being a threshold value below which the surface potential could not reach the breakdown level. As might be expected, this is somewhat higher than the value of 2.6 nA/cm^2 calculated previously[1] by ignoring the repulsive effect of accumulated surface charge. However,

experimental results already described in this paper indicate the occurrence of discharges at 0.5 nA/cm^2. One possible interpretation is that at the point of discharge initiation the incident beam has been focussed to a current density several times its measured value, and indeed some evidence exists for increased charge concentration near a specimen edge[4]. However, equation (5) is directly relevant only to punchthrough breakdown, and the observed specimen damage patterns indicate that the majority of discharges initiate at the mask edge but do not involve punchthrough. Therefore equation (5) could at best apply only to a minority of discharge arcs on masked specimens, the rest probably initiating at points of locally high near-surface fields at the mask edge.

2.10 Conclusions

Among the three dielectric materials tested, Kapton is the only one exhibiting discharge pulse characteristics which are significantly dependent on the incident electron current density. Thus previous area-scaling results[2] are valid over a wide range of current densities for Mylar and Teflon, and in the case of Kapton they can be corrected for current density dependence by using the results presented here. Thus accelerated discharge testing at high incident current densities appears to be feasible.

Indirect evidence is presented indicating that electrons from the central region of the specimen may never reach the mask. Estimation of an incident-beam current density threshold for discharge occurrence suggests that incident-beam focussing could be involved in punchthrough discharge occurrence at current densities below 4 or 5 nA/cm^2. Specimen fatigue has been noted, in the form of discharge cessation after a few arcs, and in

the form of frequent, long, low-level discharge pulses signaling the occurrence of a dielectric specimen punchthrough.

3. DIELECTRIC SURFACE DISCHARGES: EFFECTS OF COMBINED LOW-ENERGY AND HIGH-ENERGY INCIDENT ELECTRONS

3.1 Introduction

Spacecraft in synchronous orbit are exposed to a natural energetic electron flux with a continuous energy spectrum extending into the MeV range. It has been estimated that this energetic flux could penetrate the outer skin of a spacecraft and cause arc discharges to occur in interior dielectrics[5]. It has also been estimated that nuclear β-decay electrons could augment the naturally occurring high-energy electron flux by one to two orders of magnitude, thereby contributing to stronger charging or discharging phenomena[6].

Most laboratory simulations of spacecraft charging have been carried out using metal-backed dielectric sheets exposed to monoenergetic electron beams in the relatively low energy range of 15-25 keV, but recently evidence has been introduced indicating that a monoenergetic electron beam in the relatively high energy range of 200-500 keV can by itself cause discharges to occur[7] or can modify discharges caused by a simultaneously applied low-energy beam[8]. In particular it was found[8] that the addition of 200 keV electrons at 100 pA/cm^2 completely prevented the occurrence of discharges due to a 25 keV beam, even when this low energy beam's current density was as high as 13 nA/cm^2. The further investigation of this latter effect of combined high and low energy beams is the objective of the research reported here, with the primary innovation being the use of a broad-spectrum Strontium-90 high-energy β-particle source.

3.2 Experimental Conditions

In the planning stage it became clear that the experiments would be extremely time-consuming, so that the number and ranges of the parameters selected would have to be limited. Therefore it was decided to select only one set of fluxes, with the high energy flux lying very roughly between the expected natural and nuclear-enhanced values as evaluated in the literature[8], and the low energy flux large enough to permit completion of the experiments in a reasonable time. Thus the selected current densities were 10 nA/cm^2 for monoenergetic 20 keV electrons and 5 pA/cm^2 for the broad-spectrum emission from ^{90}Sr. Theoretical estimation of the emission from a 100 mCi ^{90}Sr cource indicated that a current density of 5 nA/cm^2 would exist at a distance of 3 cm from the source and Faraday cup measurements in a vacuum confirmed this estimate.

It was decided to test three materials, FEP Teflon 50 μm thick, Kapton H 50 μm thick and Mylar 75 μm thick. One reason for this choice was the existence of extensive discharge data on these three materials with respect to exposed-area scaling[2] and incident-flux scaling of the discharge peak current, released charge, energy dissipated and pulse duration (see Chapter 2). Also, Kapton was selected because of its use in previous high-energy tests, and Teflon and Mylar were chosen to reveal differences among polymers. The specimen area was kept constant at 11.7 cm^2.

It has been mentioned that discharge tests can be time-consuming. One reason for this is specimen fatigue which means that on a particular specimen discharging can suddenly stop and not recommence, or the properties of the discharges can change as the discharges continue. This means that a complete discharge history for each specimen must be recorded and the specimens changed frequently. Furthermore specimen fatigue is a property

which is as important as discharge pulse strength in assessing the effects of high-energy electron exposure.

The experimental arrangement is shown in Fig. 12. The radioisotope source was positioned so as to produce minimum blockage of the low energy beam when the low and high energy electrons were incident simultaneously. For low energy incidence alone, the radioisotope source was removed. Also shown in Fig. 12 is the emission spectrum of the high-energy source, a spectrum which exhibits a lower-energy peak due to the β-decay of ^{90}Sr to ^{90}Y, and a higher-energy peak due to the β-decay of ^{90}Y to stable ^{90}Zr.

3.3 Specimen Discharge History Examples

Each specimen was found to exhibit a particular kind and degree of fatigue as discharges recurred, and so for each specimen the discharges were assigned serial numbers. The progression of some discharge properties with serial number is shown in Fig.13 for a single Teflon specimen and low-energy electron incidence. The substrate and mask peak currents both decrease slowly for the first nine discharges, during which the waiting time between discharges increases erratically. Then there is a sudden change to lower peak currents and shorter waiting times. This type of sudden change correlates with the formation of a "punchthrough" or "pinhole" in the specimen and the subsequent arcs tend to concentrate on the punchthrough. It would appear probable that subsequent discharge arcs are initiated at the punchthrough and then propagate away from it.

The specimen time histories were organized according to serial number and the discharge properties averaged for each type of material. The example of Kapton exposed to low-energy electrons is shown in Fig. 14, in

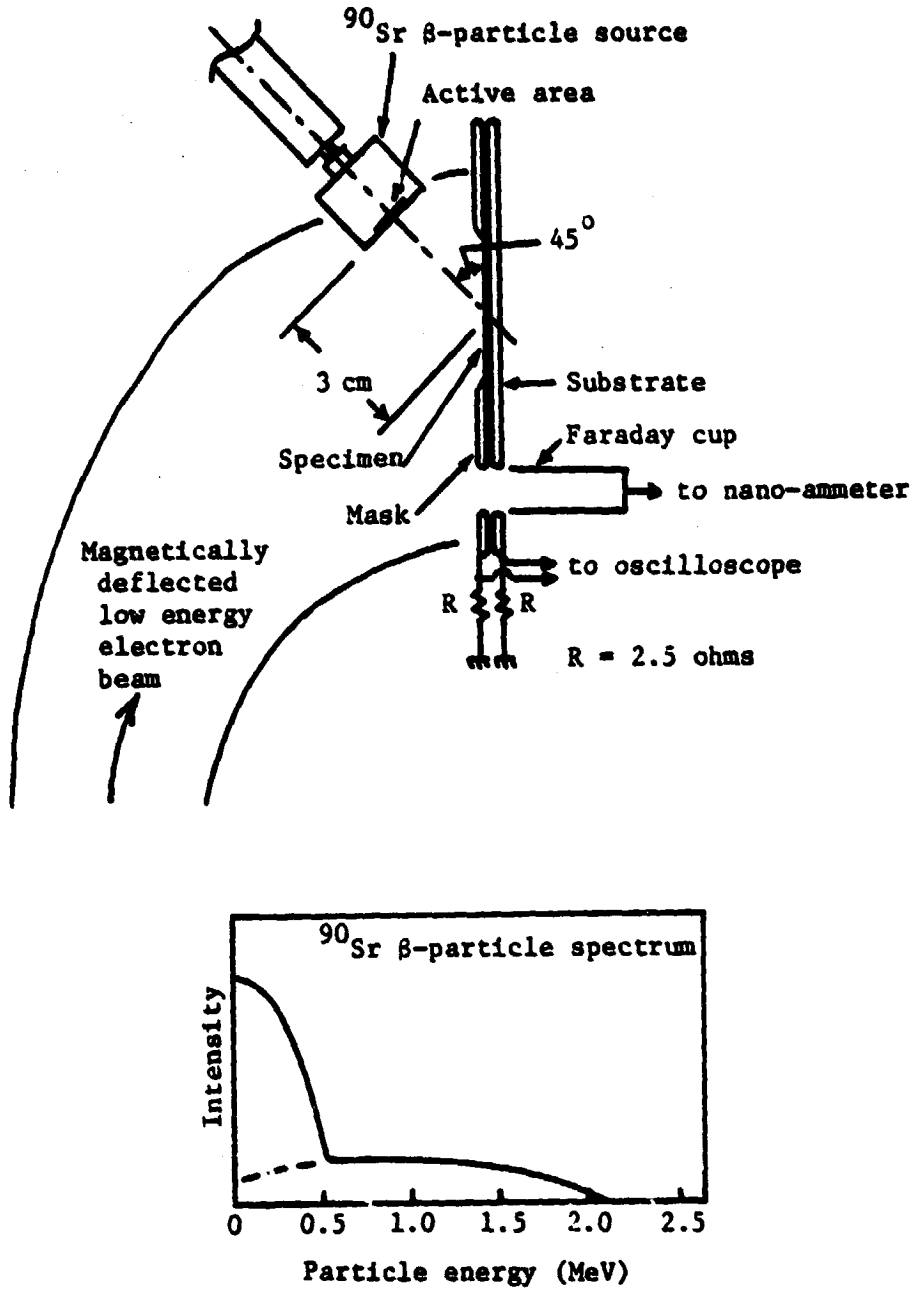

Fig.12 Experiment arrangement (a), and Strontium-90 β-particle spectrum (b). The spectrum is taken from the CRC Handbook of Radiation Measurement and Protection, p.354.

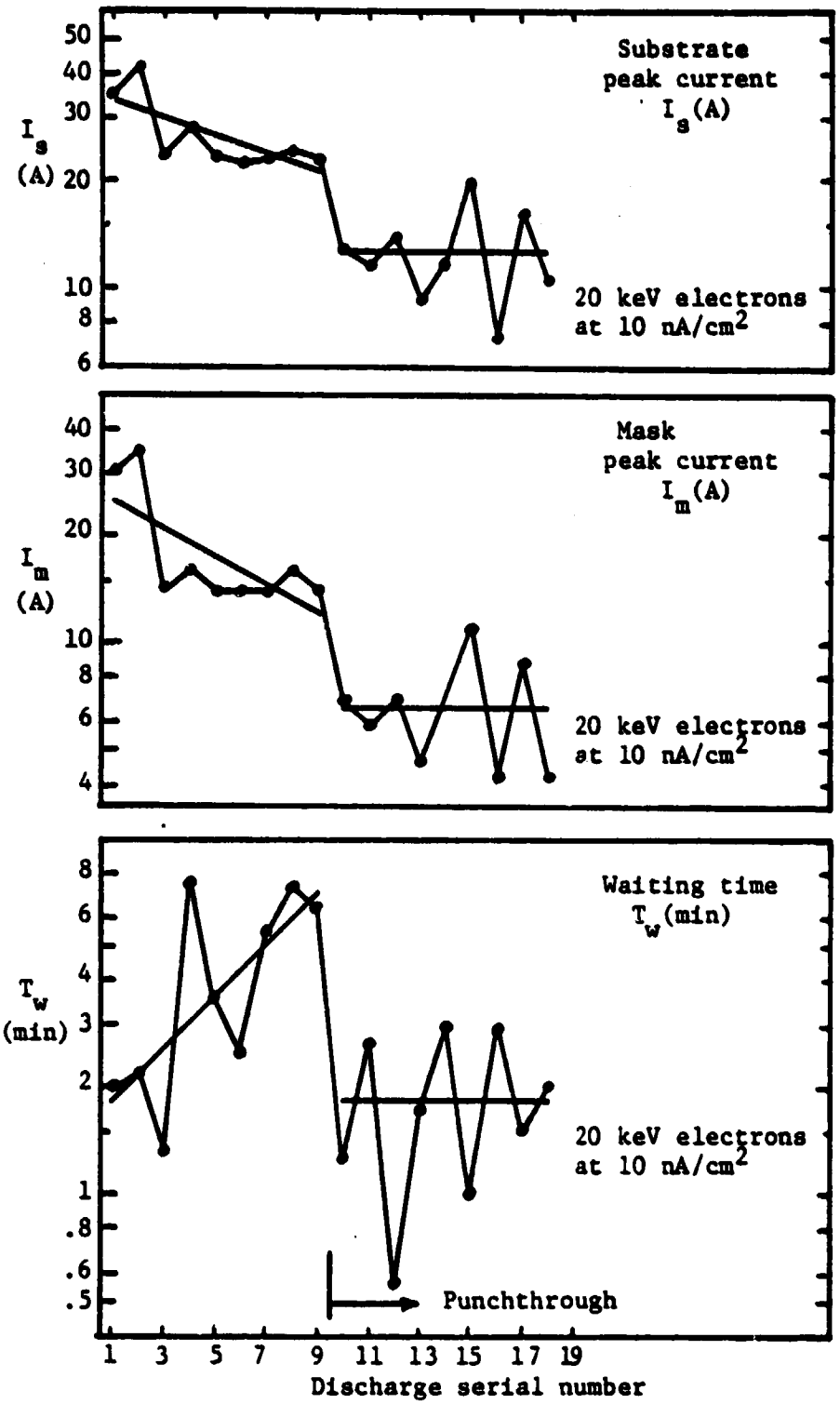

Fig.13 Discharge history of a single Teflon specimen, illustrating effects of punchthrough formation.

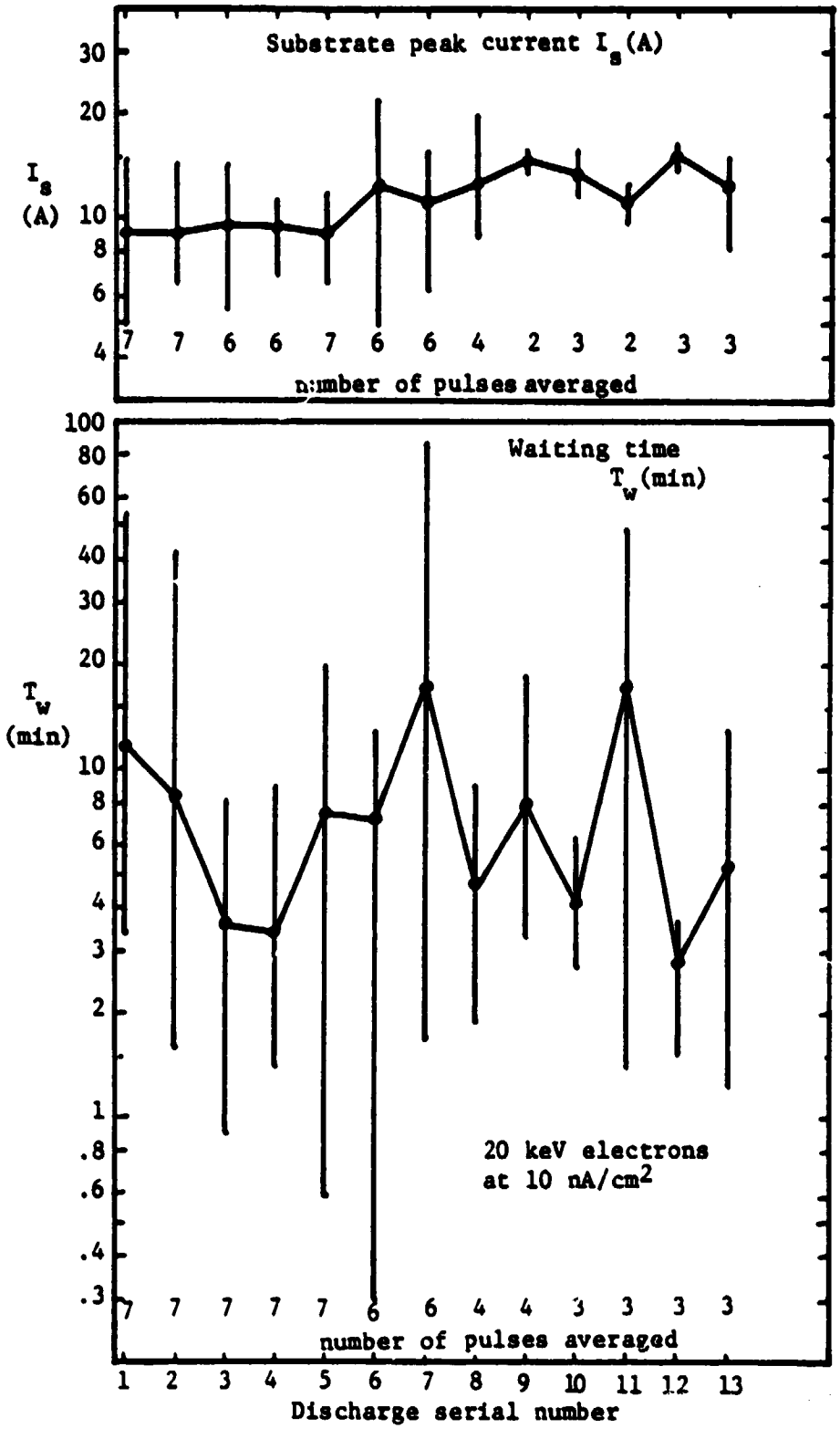

Fig.14 Average discharge history for seven Kapton specimens.

which the average peak current actually rises slightly as the discharges proceed, a process which is clearly the opposite to fatigue. The vertical bars in Fig. 14 indicate the ranges for all values measured.

As shown in Fig. 14 the waiting time exhibits a great deal of variability, indicating that the slight downward trend in the average may not be significant. It is worth noting that the longest waiting time before a discharge in this sequence was 1½ hours while the shortest was 20 seconds. Any specimen which did not discharge over a period of 1½ to 2 hours was deemed to have ceased discharging and was replaced with an unexposed specimen; some specimens did not discharge at all. In this set of experiments Kapton did not develop punchthroughs although in previous experiments on the same type and thickness of material, occasional punchthroughs did occur.

3.4 Discharge Occurrence

The periods of discharge occurrence and the points of discharge cessation are charted for the individual specimens as horizontal lines in Fig. 15. For Teflon, punchthrough-type discharge occurrence is designated by dashed lines. In the figure the vertical bar following each 6th discharge is a reminder that the computed averages of the discharge properties include only the first six discharges, and furthermore these averages exclude punchthrough-type discharges.

For Teflon the effect of adding high-energy broad spectrum electrons was to increase by 50% the number of instances of punchthrough occurrence; however the number of normal discharges per specimen remained essentially constant at about 6. For Kapton the number of discharges per specimen declined from 10 to 4.5 upon addition of the high energy electrons. For

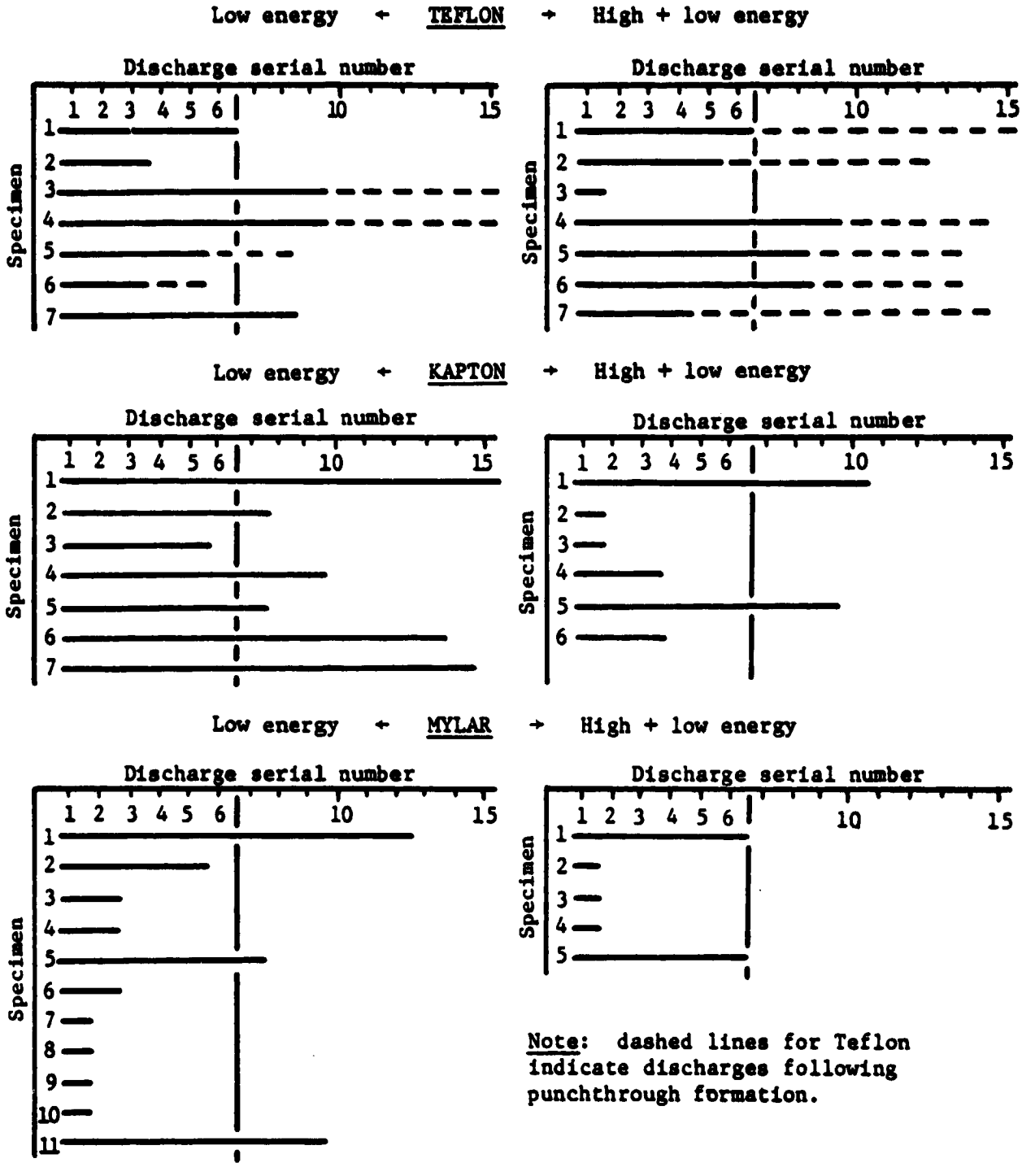

Fig.15 Discharge occurrence on individual specimens, showing effects of adding high energy electrons from strontium - 90 to a monoenergetic 20 keV beam.

Mylar the corresponding change was from 4 to 3 discharges per specimen. Clearly Kapton was the only one of the three materials to exhibit increased fatigue in the form of significantly fewer discharges per specimen upon addition of high energy electrons from the ^{90}Sr source.

3.5 Average Discharge Properties

The discharge current pulse properties were averaged over the first six normal discharges and the results depicted as bar graphs in Figs. 16, 17, 18 and 19. As for the discharge strength, Fig. 16 shows that on Teflon the addition of high energy electrons causes the peak current and released charge to decrease slightly, but has the opposite and much stronger effect on Kapton and Mylar. Indeed for Kapton the released charge is tripled and the energy dissipated (shown in Fig. 17) is multiplied by a factor of seven. The pulse durations shown in Fig. 17 are relatively unaffected by the high energy electrons.

3.6 Average Waiting Time

The increased discharge strength for Kapton and Mylar as referred to above correlates fairly well with the increased waiting time shown in Fig. 18. This correlation is better for the released charge than for the other discharge properties as can be seen in the table below.

Ratio of High + Low to Low Energy Average Discharge Properties

	I_s	Q_s	E_s	T_s	T_w
Kapton	2.6	3.0	7.1	1.2	4.1
Mylar	1.6	1.8	2.6	1.2	1.9

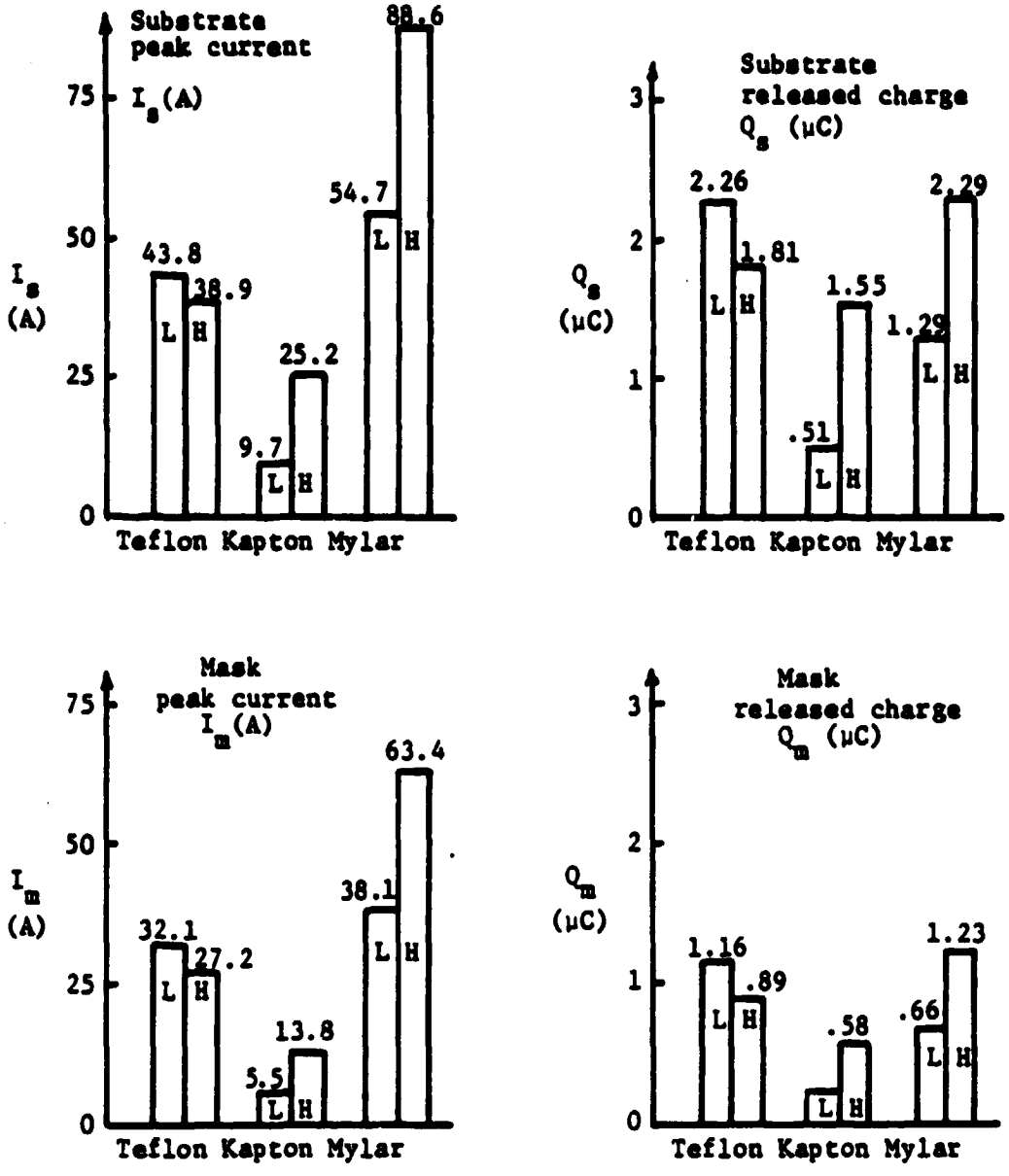

Fig.16 Average peak current and average released charge for substrate and mask as measured over first 6 discharges. L denotes low energy electron exposure and H denotes combined high and low energy exposure.

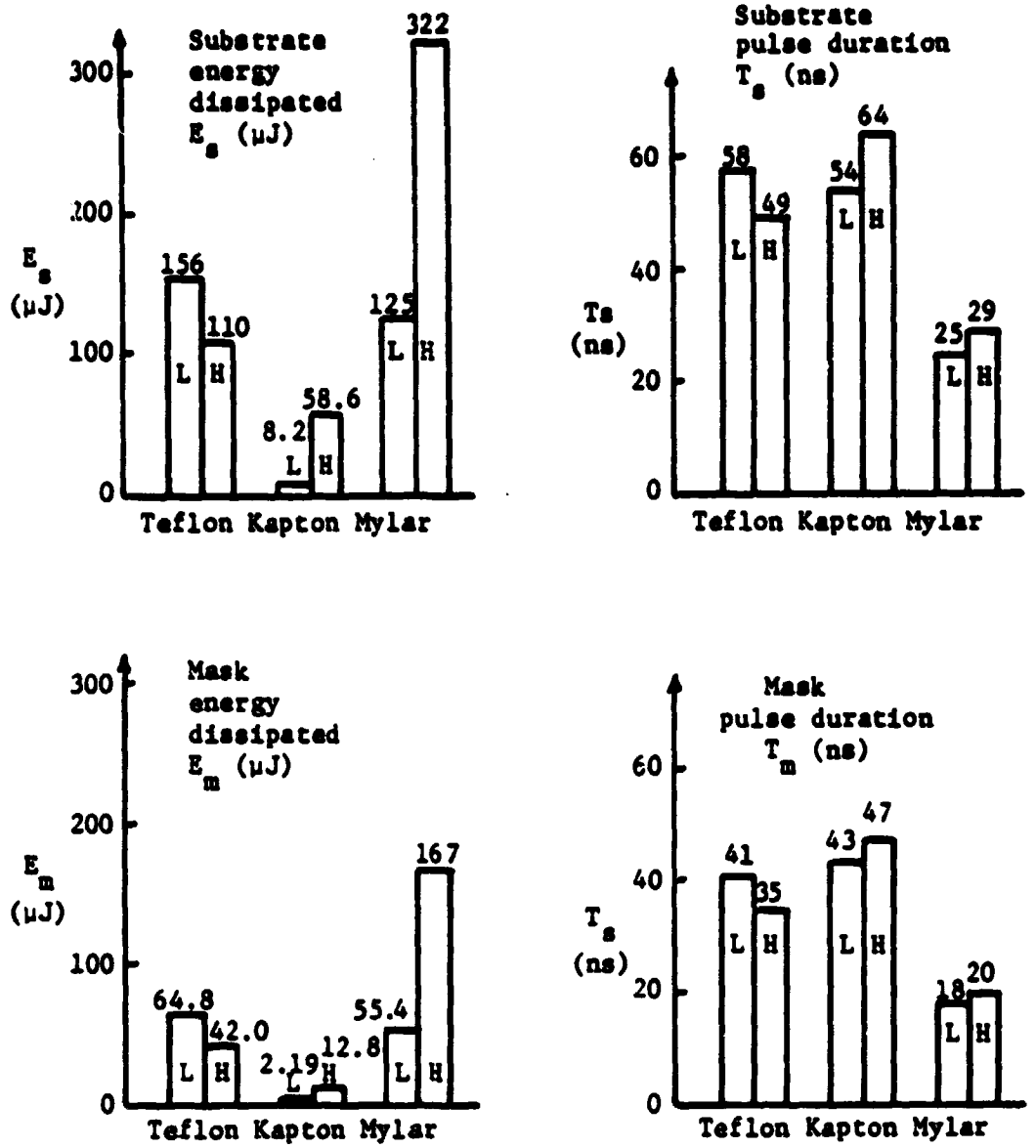

Fig. 17 Average energy dissipated in a 2.5 ohm load resistor and average pulse duration for both substrate and mask as measured over first 6 discharges. L denotes low energy electron exposure and H denotes combined high and low energy electron exposure.

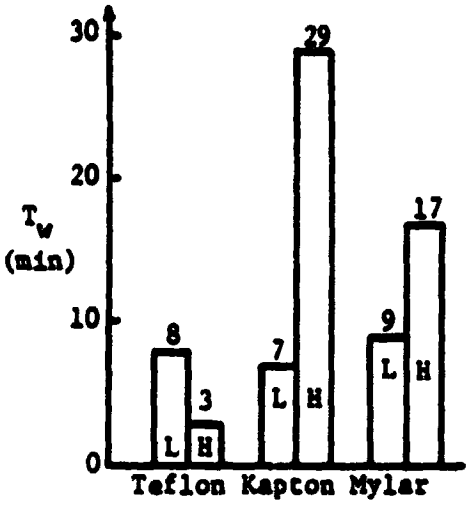

Fig.18 Average waiting time between discharges as measured over first 6 discharges. L and H denote low and combined high and low energy incident electrons.

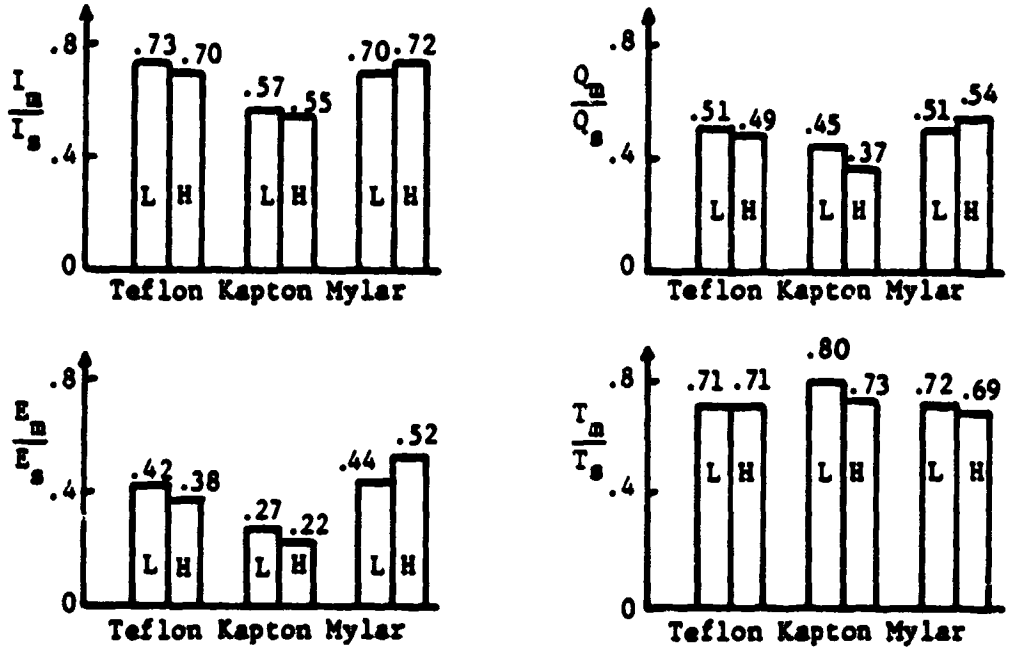

Fig.19 Average mask-to-substrate ratios over first 6 discharges for peak current, released charge, energy dissipated in a 2.5 ohm load resistor, and pulse duration.

Presumably the added high energy electrons act in some way to permit charge to build up for a longer period before discharge occurs. It is conceivable that the beam-induced conductivity allows enough charge redistribution to prevent early formation of charge concentrations and resultant breakdown-level fields. Whatever the reason may be, the factor of four increase in waiting time is particularly significant because it allows time for a much larger charge to accumulate. The longer waiting time also greatly extends the time required to perform the experiments.

The average mask-to-substrate ratios of Fig. 19 indicate that the addition of high-energy electrons has little effect. Because these ratios and also the pulse durations are so little affected, it seems reasonable to conclude that the addition of high-energy incident electrons does not affect discharge dynamics.

3.7 Trends During First Six Discharges

It is reasonable to ask whether or not the averages presented as bar graphs in Figs. 16 through 19 mask any significant variations during the first six discharges. The average discharge histories plotted in Fig. 20 address this question by showing that the peak current does not change greatly with discharge serial number, and even increases slightly in the case of Kapton for both the low energy and the combined high and low energy exposure. For specific serial numbers, the peak currents varied typically over a 2:1 range. The other discharge properties (released charge, energy, pulse duration) exhibited similar variations, indicating that the average discharge properties are indeed representative of all the discharges.

The waiting times as shown in Fig. 20 vary appreciably, with the rapid increase for Teflon exposed to low energy electrons being especially

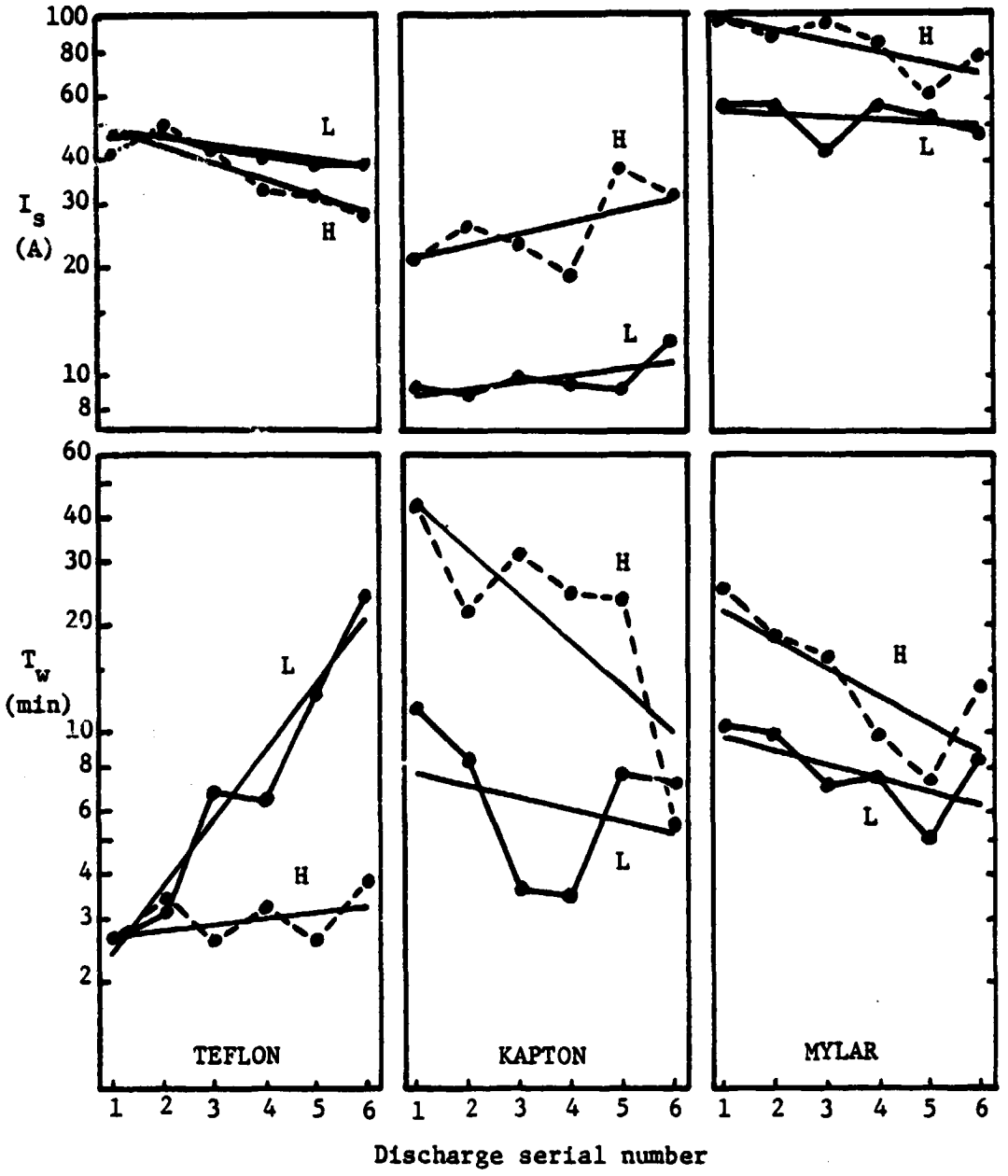

Fig.20 Average discharge histories for all specimens tested for the first 6 discharges. L and H denote low and combined high and low energy incident electrons.

noticeable. These waiting times for Teflon for a given serial number varied typically over only a 4:1 range while the averages varied over a 10:1 range, which tends to support the significance of the 10:1 variation. However no explanation is apparent. For Mylar the variation with serial number is less pronounced and probably not significant in view of the 4:1 range at a given serial number. For Kapton the situation is quite different because the variations at a given serial number were typically over a 15:1 range. In addition for the high-energy case the 6th Kapton discharge waiting time was derived from only two specimens, so consideration of all these factors suggests that the Kapton waiting time variations (decreases) over the first six discharges probably are not significant.

3.8 Conclusions

It is necessary to consider a detailed discharge history for each specimen tested in order to characterize properly each material with respect to both fatigue and average discharge properties. Such discharge histories show, for example, that the formation of a punchthrough is characterized by an abrupt change to weaker and more frequent discharges.

The addition of high-energy, broad-spectrum electrons to a 10 nA/cm^2, 20 keV electron beam has the following effects:

1. For Kapton the number of discharges per specimen is cut in half.
2. For Kapton and Mylar, the discharges that do occur are much stronger.
3. The waiting time between discharges for Kapton and Mylar increases greatly, in approximate proportion to the charge released during discharge.

4. The pulse durations and mask-to-substrate ratios remain essentially unchanged for Teflon, Kapton and Mylar.

5. For Teflon the steadily increasing waiting times for low-energy electrons become appreciably smaller and constant upon addition of high-energy electrons.

Thus for Kapton in particular, and to a lesser degree for Mylar, the effect of adding broad-spectrum high-energy incident electrons is to cause discharges which are stronger but fewer in number and less frequent. However the fact that the pulse durations and mask-to-substrate ratios are unchanged suggests that the physics of the discharge process is unaffected by the high-energy electrons. The correlation between the waiting-time and released charge suggests that the high energy electrons influence strongly the charge accumulation process. It is postulated that additional beam-induced and nonlinear conductivity during the charge-up process acts to delay the formation of charge concentrations and resultant high-field regions which are strong enough to trigger discharges.

The low-energy flux levels employed are somewhat higher than the values expected in synchronous orbit, and the ratio of low-energy to high-energy fluxes is 2000 which is also high with respect to synchronous orbit. Nevertheless conditions have been found such that discharges are made stronger by the addition of energetic electrons rather than being eliminated completely as found in earlier work done at lower low-energy fluxes[8]. Although further study is required, it is clear at this stage that the spacecraft charging threat to satellites cannot be dismissed because of the presence of high-energy electrons in synchronous orbit.

4. FIBER-OPTIC WAVE GUIDE EXPOSURE TO ELECTRON BEAMS

4.1 Introduction

It is well known that fiber-optic waveguides exhibit performance degradation under irradiation by electrons sufficiently energetic to pass through the fiber[9, 10]. However some electrons could accumulate in the fiber, in the case of partially shielded fibers on a spacecraft subjected to the broad-spectrum energetic electron environment in synchronous orbit. Conceivably these electrons might accumulate in sufficient numbers to cause electrical breakdown which would produce transient interference in the form of unwanted light emission, as well as permanent damage to the fiber. It is this question of fiber-optic waveguide discharge susceptibility which is discussed in a preliminary manner in this report.

4.2 Experimental Arrangement

Three types of fiber-optic waveguides were involved in these tests: Dupont PIFAX P-140 all-plastic, large-core fiber, Corning Corguide SDF plastic-clad silica fiber, and Corning Corguide 8020 plastic-clad silica fiber. As tested, the PIFAX had its protective jacket stripped off leaving the core and cladding, while the two Corguide fibers had core, cladding and protective coating intact.

Four configurations were employed:

a) fiber wound in a planar spiral lying on a flat metal substrate, the transient current from which could be measured as an indicator of discharge occurrence, b) fiber laid straight across the substrate and overlaid with the metal mask described in Chapters 2 and 3 of this report, c) fiber wound on a truncated aluminum cone with minimum diameter 1 cm and mounted on the

substrate, and d) end-on exposure of a single fiber to the beam, with the fiber protruding through a hole in the substrate.

Light propagating along the fiber was measured using an RCA C30908E avalanche photodiode connected through a preamplifier to a 400 MHz bandwidth oscilloscope. This system was tested by using it to measure the transient light emitted by a planar-dielectric discharge; this light was found to persist for a time period somewhat longer than the substrate pulse.

Both low energy and high energy incident electron beams were employed. The low energy beam consisted of 20 keV monoenergetic electrons and the high energy beam consisted of the broad-spectrum β-particle emission from the ^{90}Sr radioisotope source described in Chapter 3.

4.3 Results for PIFAX P-140

A 127 cm length of PIFAX P-140 in the planar spiral configuration was exposed to low energy electrons at 100 nA/cm^2 for 3 hours and at 300 nA/cm^2 for 5 min with no discharge, but when the beam was turned off, a 2.5A discharge occurred. A new 250 cm long planar spiral of fiber was then exposed for 5 hours at 250 nA/cm^2 with no discharge. As a result of the electron bombardment, both specimens turned yellowish-brown.

In the end-on low-energy exposure configuration, the PIFAX P-140 showed faint visible luminescence but it was too weak to be detected by the avalanche photodiode. In 2 3/4 hours of exposure to low energy electrons at 200 nA/cm^2, no discharges were observed. In the end-on high-energy exposure configuration, one hour of exposure produced neither discharges nor visible luminescence.

When wrapped on the aluminum cone, the PIFAX P-140 did not discharge during a 45 min exposure to low energy electrons at 300 nA/cm^2. The current density was then raised to a higher value (which could not be measured),

after which there was bright luminescence, discharge arcs occurred at a rate of about one per second, and light pulses were detected at the end of the fiber. The current density was then restored to 300 nA/cm^2 and this time the discharges continued as did the corresponding light pulses. The fiber was discoloured and showed small surface cracks.

4.4 Results for Corguide SDF

A 208 cm flat spiral of Corguide SDF was exposed to low energy electrons at 50 nA/cm^2 for one hour without discharging although light blue luminescence was visible. At 250 nA/cm^2 a few discharges of about 2A peak current were recorded although no light pulses were detected by the avalanche photodiode in spite of the fact that a rather diffuse flash could be seen at each discharge.

A straight piece of Corguide SDF held down by the circular-aperture mask did not discharge under low energy exposure at 250 nA/cm^2 but a second specimen did under the same conditions. A total of 22 pulses were then recorded over incident current densities varying in 5 steps from 300 to 10 nA/cm^2. The peak substrate discharge currents averaged about 40 mA (ranging from 17 to 95 mA) and showed no conclusive evidence of flux scaling. Also, no light pulses were detected. The waiting time between discharges varied from 1 to 10 minutes.

When high energy electrons were added to the low energy exposure experiment with Corguide SDF fiber as described above, discharges were observed but no light pulses were detected. The average peak substrate current over 26 discharges went from 33 mA to 14 mA as the incident current density was changed in 4 steps from 300 to 20 nA/cm^2 so it could be said that some flux scaling was measured. Furthermore the additional

high energy exposure caused the average peak discharge current to drop by a factor of about 2.

In the end-on configuration, the Corguide SDF was exposed to low energy electrons at 300 nA/cm^2 for 3/4 hr. No discharges were observed.

A 70 cm length of Corguide SDF was wrapped on the aluminum cone and exposed to low energy electrons. For incident current densities in the range of 200 to 300 nA/cm^2 discharges with peak currents of the order of 20 mA were observed.

4.5 Results for Corguide 8020

A straight piece of Corguide 8020 held down by the mask was exposed to low energy electrons at 300 nA/cm^2. Discharges were observed with a peak current of 17 mA.

A 60 cm length of Corguide 8020 was wound on the cone. After $1\frac{1}{2}$ hr. of exposure to low energy electrons at 200 nA/cm^2 no discharge had been observed. Raising the incident current density to over 300 nA/cm^2 caused bright luminescence and bright flashes accompanying discharges with peak currents of about 30 mA. The fiber then turned yellow and broke in two places.

4.6 Conclusions

For the conical spiral arrangement and low energy exposure, no discharges were observed below an incident current density of 200 nA/cm^2. For end-on exposure no discharges were observed under any conditions including exposure to high energy electrons. For the flat spiral arrangement, discharges were observed only on Corguide SDF and then only at 250 nA/cm^2. Thus in these cases which involved no sharp edges in contact with the fiber, only extremely strong electron bombardment produced discharges.

In those configurations involving a straight fiber held down by a metal mask, the sharp edge of the mask was in contact with the fiber. Under these conditions discharges were observed for incident current densities as low as 10 nA/cm^2 on Corguide SDF, and weaker discharges were observed down to 20 nA/cm^2 in the presence of additional high-energy electrons.

Only in the case of PIFAX P-140 wound on a cone were light pulses detected at the end of the fiber-optic waveguide, and this only for incident current densities over 300 nA/cm^2. This is not too surprising because PIFAX P-140 has very thin cladding, and for the other materials the deposited charge did not penetrate the cladding deeply enough to permit discharge light coupling into the core.

5. REFERENCES

1. Flanagan, T.M., Denson, R., Mallon, C.E., Treadaway, M.J., and Wenaas, E.P., "Effect of Laboratory Simulation Parameters on Spacecraft Dielectric Discharges," IEEE Trans. Nucl. Sci., Vol. NS-26, No. 6, Dec. 1979, pp. 5134-5140.

2. Balmain, K.G., and Dubois, G.R., "Surface Discharges on Teflon, Mylar and Kapton", IEEE Trans. Nucl. Sci., Vol. NS-26, No. 6, Dec. 1979, pp. 5146-5151.

3. Stevens, N.J., Berkopek, F.D., and Blech, R.A., NASA TMS-73436, June 1976.

4. Balmain, K.G., "Scaling Laws and Edge Effects for Polymer Surface Discharges", in Spacecraft Charging Technology 1978, NASA Conference Publication 2071/AFGL-TR-79-0082, pp. 646-656.

5. Wenaas, E.P., "Spacecraft Charging Effects by the High-Energy Natural Environment", IEEE Trans. Nucl. Sci., Vol. NS-24, No. 6, Dec. 1977, pp. 2281-2284.

6. De Plomb, E.P., and Rich, W.F., "Charging of Spacecraft by Nuclear Electrons", IEEE Trans. Nucl. Sci., Vol. NS-24, No. 6, Dec. 1977, pp. 2298-2304.

7. Wenaas, E.P., Treadaway, M.J., Flanagan, T.M., Mallon, C.E., and Denson, R., "High-Energy Electron-Induced Discharges in Printed Circuit Boards", IEEE Trans. Nucl. Sci. Vol. NS-26, No. 6, Dec. 1979, pp. 5152-5155.

8. Treadaway, M.J., Mallon, C.E., Flanagan, T.M., Denson, R., and Wenaas, E.P., "The Effects of High-Energy Electrons on the Charging of Spacecraft Dielectrics", IEEE Trans.Nucl. Sci.

Vol. NS-26, No. 6, Dec. 1979, pp. 5102-5106.

9. Friebele, E.J., Jaeger, R.E., Sigel, G.H., and Gingerich, M.E., "Effect of Ionizing Radiation on the Optical Attenuation in Polymer-Clad silica Fiber-Optic Waveguides", Appl. Phys. Lett. Vol. 32, No.2, 15 Jan. 1978, pp. 95-97.

10. Landry, M.J., Davis, H.P., "Electron-Beam Induced Absorption and Hardening in Fiber-Optic Waveguides to 1060 nm Laser Pulses", Report SAND 79-1208, Sandia Laboratories, July 1979.